

THE PHYSICAL REVIEW

A journal of experimental and theoretical physics established by E. L. Nichols in 1893

SECOND SERIES, VOL. 168, No. 4

20 APRIL 1968

Two-Body Photodisintegration of He^3 [†]

N. J. CARRON

Department of Physics, University of Illinois, Urbana, Illinois 61801

(Received 13 October 1967)

A discussion and comparison of the two forms of interaction, $\mathbf{A} \cdot \mathbf{p}$ and $\mathbf{E} \cdot \mathbf{r}$, is given for two-body photodisintegration of He^3 . It is shown that in general the $\mathbf{E} \cdot \mathbf{r}$ results are much better than the $\mathbf{A} \cdot \mathbf{p}$ results. Calculations are carried out to 140 MeV to compare with recent data. The Gunn-Irving wave function gives a good fit to the total cross section at all energies, but fails to account for the ground-state matter form factor. A simple three-nucleon ground-state wave function is suggested which adequately reproduces the Coulomb energy, rms radius, and matter form factor (for $q^2 \lesssim 3.5 \text{ F}^{-2}$) of He^3 , but predicts a photodisintegration cross section which is 20% small at the peak, assuming no final-state interactions. The spin magnetic-moment interaction, which Verde has shown is forbidden in the dipole approximation for transitions from a spatially symmetric ground state, is computed without this approximation and is shown to contribute only 1–10% of the total cross section, the larger amount only at high energies.

I. INTRODUCTION

THERE have been several calculations of the photodisintegration of the three-nucleon system.^{1–9} These have been primarily of the total cross sections for photon energies $\lesssim 40$ MeV, and calculated in the dipole approximation, although recently authors have included quadrupole terms. [There are four processes: $\text{H}^3(\gamma, n)d$, $\text{H}^3(\gamma, p)2n$, $\text{He}^3(\gamma, n)2p$, $\text{He}^3(\gamma, p)d$. In this paper we concentrate on the last case.] In the present paper we compare the two forms of interaction $\mathbf{A} \cdot \mathbf{p}$ and $\mathbf{E} \cdot \mathbf{r}$ for the photon-nucleus interaction and carry out calculations up to 140 MeV, to compare with recent data.

In order to evaluate the transition matrix element, one needs to choose an appropriate initial wave function for the three-nucleon ground state; one must decide on the proper form of interaction between the external electromagnetic field and the nuclear charge-current

system, and one must choose the correct final wave function of the three nucleons.

Regarding the initial ground state: The theoretical work done on determining this state has concentrated primarily on reproducing the ground-state properties such as Coulomb energy, binding energy, rms radius, and form factor.^{10–15} From this work, it is clear that the predominant state is the spatially symmetric S state times the antisymmetric doublet spin state. There is some question as to the amount of D state and/or mixed symmetry S' state present,¹⁶ but it is no more than a few percent. For our purposes we consider only the doublet spin state and choose an appropriate symmetric wave function as discussed in Sec. II.

Regarding the photon-nucleus interaction: The nucleus is a charge-current distribution $j_\mu = (\mathbf{j}, \rho)$ interacting with a (known) external field $A_\mu = (\mathbf{A}, \varphi = 0)$. The interaction Hamiltonian (density) is

$$V = -(1/c)j_\mu A_\mu = -(1/c)\mathbf{j} \cdot \mathbf{A}.$$

But \mathbf{j} is not known, for there are meson currents in the nucleus which contribute to the total electromagnetic current of the nucleus, and an ordinary Schrödinger

[†] This work was supported by the National Science Foundation under Grant Nos. NSF-GP 2799 and NSF-GP 6198.

¹ M. Verde, *Helv. Phys. Acta* **23**, 453 (1950).

² J. C. Gunn and J. Irving, *Phil. Mag.* **42**, 1353 (1951).

³ L. M. Delves, *Nucl. Phys.* **29**, 268 (1962).

⁴ U. Eichmann, *Z. Physik* **175**, 115 (1963).

⁵ R. I. Dzhibuti, V. I. Mamasakhlisov, and T. S. Macharadze, *Yadern. Fiz.* **2**, 59 (1965) [English transl.: *Soviet J. Nucl. Phys.* **2**, 40 (1966)].

⁶ V. N. Fetisov, *Zh. Eksperim. i Teor. Fiz.* **46**, 1395 (1964) [English transl.: *Soviet Phys.—JETP* **19**, 943 (1964)].

⁷ G. M. Bailey, G. M. Griffiths, and T. W. Donnelly, *Nucl. Phys.* **A94**, 502 (1967).

⁸ B. F. Gibson, *Nucl. Phys.* **B2**, 501 (1967).

⁹ R. Bösch, J. Lang, R. Müller, and W. Wölfl, *Helv. Phys. Acta* **38**, 753 (1965).

¹⁰ H. Collard, R. Hofstadter, E. B. Hughes, A. Johansson, M. R. Yearian, R. B. Day, and R. T. Wagner, *Phys. Rev.* **138**, B57 (1965).

¹¹ B. F. Gibson, *Phys. Rev.* **139**, B1153 (1965).

¹² B. F. Gibson and L. I. Schiff, *Phys. Rev.* **138**, B26 (1965).

¹³ L. I. Schiff, *Phys. Rev.* **133**, B802 (1964).

¹⁴ J. Pappademos, *Nucl. Phys.* **42**, 122 (1963); **56**, 351 (1964).

¹⁵ R. H. Dalitz and T. W. Thacker, *Phys. Rev. Letters* **15**, 204 (1965).

¹⁶ B. F. Gibson and L. I. Schiff, *Phys. Rev.* **138**, B26 (1965).

wave function (a function of the three positions of the nucleons), such as we are using, of course does not take into account these (virtual) mesons. In a nonrelativistic Schrödinger treatment, one can approximate the effect of the pions by inserting a "charge-exchange" potential in the nuclear Hamiltonian (which potential is then a phenomenological description of mesons) and solve for the nuclear ground-state wave function in its presence. Thus the mesons affect the ground state, and also, via their electromagnetic current, affect the interaction of the nucleus with an external field. At any rate the current is not just the convection current

$$\sum_{i=1}^Z \frac{e}{M} \mathbf{p}_i$$

of Z point protons. Thus $V = -\sum_i (e/Mc) \mathbf{A} \cdot \mathbf{p}_i$ is not completely correct.

Now at low energies one might expect the dipole approximation to hold, as it does in atomic physics. In the nuclear-dipole approximation, there are three separate approximations involved:

1. Replace $\mathbf{A} = A_0 \boldsymbol{\varepsilon} e^{i\mathbf{k} \cdot \mathbf{r}}$ by $A_0 \boldsymbol{\varepsilon} = \mathbf{A}_0$, where $\boldsymbol{\varepsilon}$ is the photon polarization vector.
2. Replace \mathbf{p} by $M\mathbf{v} = (M/i\hbar)[H, \mathbf{r}]$ so that

$$\langle f | \mathbf{A} \cdot \mathbf{p} | i \rangle \rightarrow A_0 \boldsymbol{\varepsilon} (M/i\hbar) \cdot \langle f | [H, \mathbf{r}] | i \rangle,$$

where H is the unperturbed nuclear Hamiltonian.

3. Apply H to $|f\rangle$ and $|i\rangle$ and bring out $(E_f - E_i)$ so that

$$\langle f | \mathbf{A} \cdot \mathbf{p} | i \rangle \rightarrow -iM\omega A_0 \boldsymbol{\varepsilon} \cdot \langle f | \mathbf{r} | i \rangle,$$

where $\hbar\omega = (E_f - E_i)$. Since $\omega A_0 \boldsymbol{\varepsilon}$ is proportional to the electric field \mathbf{E}_0 , one is effectively evaluating $\langle f | \mathbf{E}_0 \cdot \mathbf{r} | i \rangle$.

Step 1 is certainly legitimate at low energies. In atomic physics steps 2 and 3 do not really involve any approximation; they are identically correct (assuming the atomic eigenstates are known). However, in the nuclear case, step 2 requires that the internal nuclear potential commute with the nucleon position \mathbf{r} . This is not the case if a charge-exchange potential is included. Thus, in nuclear physics, step 2 is not valid unless one makes specific allowance for the commutator of the exchange potential. Step 3 requires that $|i\rangle$ and $|f\rangle$ be true eigenstates of a nuclear Hamiltonian corresponding to eigenvalues differing by $\hbar\omega$. For any states used in a calculation, this is generally not the case. The wave functions are chosen on plausibility grounds and are not true eigenstates of a single Hamiltonian. In fact $|i\rangle$ and $|f\rangle$ may not even be orthogonal. Thus step 3 is not valid in a calculation. With the use of inexact wave functions we may expect the two forms of interactions to give different results.¹⁷

¹⁷ This is discussed in the atomic case in H. A. Bethe and E. E. Salpeter, *Quantum Mechanics of One and Two Electron Atoms* (Academic Press Inc., New York, 1957), Sec. 59.

The point is that although at first sight (allowing approximation 1) $\mathbf{A}_0 \cdot \mathbf{p}$ and $\mathbf{E}_0 \cdot \mathbf{r}$ should yield nearly the same result at low energies, we now see that they need not. In fact they do not. They are both calculated here and compared. In general the interaction $\mathbf{E} \cdot \mathbf{r}$ gives a better fit to the data whereas the $\mathbf{A} \cdot \mathbf{p}$ results are all small.

We also find that much better agreement is found (particularly at high energies) if in the $\mathbf{E} \cdot \mathbf{r}$ interaction we include the retardation factor $e^{i\mathbf{k} \cdot \mathbf{r}}$ instead of using a constant electric field. These two different cases are compared below. The second term in the Taylor series expansion of $e^{i\mathbf{k} \cdot \mathbf{r}}$ contains the electric quadrupole contribution (as well as the magnetic dipole). The fact that inclusion of this term has a pronounced effect upon the cross section was also observed by Eichmann,⁴ who employed a direct multipole expansion of the field, and by Bailey *et al.*⁷

Foldy¹⁸ and Sachs and Austern¹⁹ have given a theoretical basis for retaining the factor $e^{i\mathbf{k} \cdot \mathbf{r}}$ in the electric interaction. The latter authors base their development on gauge invariance of electromagnetic interactions, while the former author bases his arguments on the differential charge conservation law. Actually, Foldy suggests an average

$$\int_0^1 ds e^{is\mathbf{k} \cdot \mathbf{r}}$$

over the retardation factor. If this average is performed in the matrix elements, the resulting cross section is intermediate between the pure dipole results ($e^{i\mathbf{k} \cdot \mathbf{r}} = 1$) and our results quoted with the full $e^{i\mathbf{k} \cdot \mathbf{r}}$.

One might expect a three-nucleon wave function to represent the charge distribution of the nucleus more nearly correctly than the current distribution, since it does give the nucleon positions but makes no reference to the motion of exchanged charged mesons. Thus, it is not surprising that $\langle f | \mathbf{E} \cdot \mathbf{r} | i \rangle$, which is like the matrix element of a charge distribution, gives better results than $\langle f | \mathbf{A} \cdot \mathbf{p} | i \rangle$, which is more like the matrix element of a current.

In addition there is a small flip interaction, $-\mathbf{m} \cdot \mathbf{B}$, of the magnetic field \mathbf{B} , with the nucleon magnetic moments \mathbf{m} . This is indeed small. We find that it accounts for only about 1% of the total cross section below 40 MeV and about 10% between 100 and 140 MeV, provided we properly orthogonalize the initial and final three-nucleon states. (Otherwise the contribution would be from 10-50% of the total cross section.) It was long ago noticed by Schiff,²⁰ and later by Verde¹ that in the dipole approximation (meaning only step 1 above) this magnetic dipole transition is forbidden if the ground state is spatially symmetric.

¹⁸ L. L. Foldy, Phys. Rev. **92**, 178 (1953).

¹⁹ R. G. Sachs and N. Austern, Phys. Rev. **81**, 705 (1951); N. Austern and R. G. Sachs, *ibid.* **81**, 710 (1951).

²⁰ L. I. Schiff, Phys. Rev. **52**, 242 (1937).

In this approximation \mathbf{B} is a constant vector and may be taken out of the matrix element, leaving only the spinor operator \mathbf{m} between initial and final spin states but no operator between initial and final spatial states. By orthogonality, therefore, the matrix element vanishes. This is seen in our expression (7) for the matrix element when we set $e^{i\mathbf{k}\cdot\rho_j}$ (the spatial dependence of the magnetic field) equal to 1.

Thus we consider three separate interactions, $\mathbf{A}\cdot\mathbf{p}$, $\mathbf{E}\cdot\mathbf{r}$, and $\mathbf{m}\cdot\mathbf{B}$, and present the results in the next two sections.

Regarding the final state: For the wave function of the deuteron we employ the triplet spin state and the Hulthén function

$$U_D(\mathbf{r}) = N_D(e^{-\alpha r} - e^{-\beta r})/r,$$

where r is the separation of the neutron and proton, $\alpha = (ME_B)^{1/2} = 45.7$ MeV/ c , and $\beta = 260$ MeV/ c .²¹

For the relative proton-deuteron motion, it has been calculated^{22,23} that final-state interactions play a small role. P -wave proton-deuteron phase shifts are known to be small.²² Thus we use a plane wave for this relative motion. However, to investigate the qualitative effects of a final-state interaction, we discuss in Sec. III the effect of a spherical square-well interaction between proton and deuteron, and the possible effect of a deuteron whose size depends on the distance of the free proton. This last notion arises because in He^3 the proton and neutron which are to become the deuteron are more tightly bound to each other when the second proton is present than they are when this second proton is free and far away. That is, the nucleon separation in the deuteron is larger than the separation of any two nucleons in He^3 . Thus, as the free proton exists from the helium, the remaining two nucleons are actually closer together than our final-state deuteron wave function gives them credit for.

In view of other uncertainties and the fact that $\mathbf{E}\cdot\mathbf{r}$ emphasizes large distances, the effect of a hard core in the initial and final states has not been considered. Indeed, Fetisov has shown⁶ that such a core produces only a small change in the results of Gunn and Irving.² Other authors^{8,24} have considered a soft or hard core in photo- and electrodisintegration.

Of the recent helium photodisintegration calculations, Dzhibuti *et al.*⁵ tried the interaction $\mathbf{A}\cdot\mathbf{p}$ (with \mathbf{A} a constant), using the Gunn-Irving ground state and $r^{-1}e^{-\alpha r}$ for the deuteron. They used a helium parameter $\mu^{-1} = 2.0$ F on the basis of a variational binding-energy calculation, but, as we shall see in the next section, this value is in wild disagreement with the Coulomb energy and form-factor data. As the cross section is sensitive

to the shape of the deuteron, the use of a Hulthén function would produce quite different results.

Eichmann⁴ and Bosch *et al.*⁹ have performed a more elaborate computation, keeping dipole and quadrupole interactions and including nonsymmetric terms in the ground state. Their results show that the nonsymmetric contribution shifts the peak to lower energy but does not greatly affect the integrated cross section (to 30 MeV). The inclusion of the quadrupole interaction has a pronounced effect on the angular distribution of He^3 disintegration: It pushes the peak of the distribution farther forward from 90° to 70° – 75° at 15 MeV. The effect of the final-state interaction is to increase the peak cross section (which occurs at about 11 MeV) by about 20% but to slightly decrease the cross section above 25 MeV.

These same effects will be observable in the present calculation. We discuss the alternative forms for the electromagnetic interaction, and suggest a very simple wave function which adequately reproduces the Coulomb energy and form factor (and therefore the rms radius) of the ground state.

There are substantial experimental data for total cross sections and 90° cross sections for helium photodisintegration.^{9,25–33} Results prior to 1965 are nicely summarized in Ref. 26. Our graphs use a representative sample of this data. There are now also recent results²⁸ on total and differential cross sections up to 140 MeV.

II. CHOICE OF WAVE FUNCTION AND CALCULATION

We now discuss the choice of the ground-state wave function and evaluation of the photodisintegration cross section.

We use the three functions

$$\Psi_1 = N_G \exp(-\mu^2 R^2), \quad (1)$$

$$\Psi_2 = N_{GI} [\exp(-\mu R)]/R, \quad (2)$$

$$\Psi_3 = N [\exp(-\mu_1 R) - \exp(-\mu_2 R)]/R, \quad (3)$$

$$R = \left(\sum_{i < j} r_{ij}^2 \right)^{1/2}.$$

²⁵ T. A. Varfolomeev and A. N. Gorbunov, Zh. Eksperim. i Teor. Fiz. **47**, 30 (1964) [English transl.: Soviet Phys.—JETP **20**, 20 (1965)].

²⁶ J. R. Stewart, R. C. Morrison, and J. S. O'Connell, Phys. Rev. **138**, B372 (1965).

²⁷ B. L. Berman, L. J. Koester, and J. H. Smith, Phys. Rev. **133**, B117 (1964).

²⁸ N. M. O'Fallon, L. J. Koester, and J. H. Smith (to be published).

²⁹ A. N. Gorbunov and A. T. Varfolomeev, Phys. Letters **11**, 137 (1964).

³⁰ V. N. Fetisov, A. N. Gorbunov, and A. T. Varfolomeev, Nucl. Phys. **71**, 305 (1965).

³¹ A. N. Gorbunov and A. T. Varfolomeev, Phys. Letters **5**, 149 (1963).

³² E. Finckh, R. Kosiek, K. H. Lindenberger, U. Meyer-Berkhout, N. Nücker, and K. Schlüpmann, Phys. Letters **7**, 271 (1963).

³³ J. B. Warren, K. L. Erdman, L. P. Robertson, P. A. Axen, and J. R. MacDonald, Phys. Rev. **132**, 1691 (1963).

²¹ D. H. White, R. N. Schectman, and B. M. Chasan, Phys. Rev. **120**, 614 (1960).

²² B. H. Bransden, A. C. Douglas, and H. H. Robertson, Phil. Mag. **2**, 1211 (1957).

²³ R. S. Christian, J. L. Gammel, Phys. Rev. **91**, 100 (1953).

²⁴ F. C. Khanna, Nucl. Phys. **A97**, 417 (1967).

The Gaussian (1) does not have the correct asymptotic behavior to satisfy the Schrödinger equation at large separations, and we shall see that the low-energy peak occurs at too high an energy, and at high energies ($\gtrsim 90$ MeV) it drops off too rapidly. The Gunn-Irving function (2) has a singularity at the origin which produces a too large form factor at high q^2 . In Eq. (3) we have subtracted out this singularity. This is not meant to introduce a nucleon core as done by Gibson⁸ and Khanna,²⁴ since Ψ_3 is nonzero at the origin, but only to make the wave function finite.

To determine values for the parameters μ and μ_1, μ_2 we calculate the matter form factor and Coulomb energy for He^3 with each function.

For the form-factor calculation and in the photo-disintegration matrix elements, the usual procedure is to introduce, in place of the nucleon coordinates $\mathbf{r}_1, \mathbf{r}_2, \mathbf{r}_3$, the internal coordinates $\boldsymbol{\rho} = \mathbf{r}_1 - \frac{1}{2}(\mathbf{r}_2 + \mathbf{r}_3)$ and $\mathbf{s} = \sqrt{3/2}(\mathbf{r}_3 - \mathbf{r}_2)$ and the center-of-mass position $\mathbf{R} = \frac{1}{3}(\mathbf{r}_1 + \mathbf{r}_2 + \mathbf{r}_3)$.

The form factor

$$F(q^2) = \int d\tau e^{i\mathbf{q}\cdot\boldsymbol{\tau}} |\psi(\boldsymbol{\rho}, \mathbf{s})|^2,$$

where $\mathbf{r} = \frac{2}{3}\boldsymbol{\rho}$, $d\tau = d^3\rho d^3s$ for the three wave functions, is shown plotted in Fig. 1. (Analytic expressions are given in the Appendix.) Two values of μ , determined by Coulomb energy and rms radius, are shown for ψ_1 and ψ_2 . Curves a and b (straight lines on this semilog plot) are for the Gaussian. Curves d and e are the Gunn-Irving. Curve c is ψ_3 for the values $1/\mu_1 = 1.9$ F, $\mu_2 = 1.44\mu_1$, which we find gives the best fit. The experimental points shown are $F_{\text{CH}}(\text{He}^3)$ (from Ref. 10) divided by $(G_B^p + \frac{1}{2}G_B^n)$ (Ref. 34).

For the Gaussian, the Coulomb value (b) yields a form factor which is everywhere too large, whereas the rms value (a) fits only the low q^2 data and is then too small.

The Gunn-Irving gives the wrong shape. No value of μ fits the data for any significant range of q^2 . The rms value (e) agrees only for the smallest q^2 and then swings far too high. The Coulomb value (d) is too small for small q^2 and then again swings too high.

Wave function (3) gives an excellent fit (c) for all $q^2 \lesssim 3f^{-2}$ and then again is too high. Its initial slope is slightly too negative, which gives it a slightly large rms radius [$F(q^2) \approx 1 - \frac{1}{6}q^2\langle r^2 \rangle$ for small q^2].

The experimental binding energy difference between He^3 and H^3 is 0.764 MeV. If we ignore proton structure, the Coulomb energy $E_c = \langle \psi | e^2/r_{12} | \psi \rangle$ is easy to calculate. The Coulomb energy parameter values in Fig. 1 were obtained by equating this to the binding energy difference, a procedure which has been questioned by Okamoto.³⁵ For the set of values of μ_1, μ_2 used in the

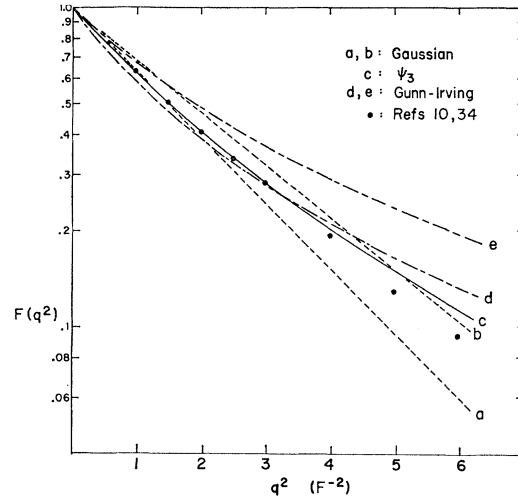


FIG. 1. He^3 matter form factor. Curve (a), Gaussian, $\mu^{-1} = 4.1$; (b) Gaussian, $\mu^{-1} = 3.684$; (c) Ψ_3 , $\mu_1^{-1} = 1.9$, $\mu_2 = 1.44\mu_1$; (d) Gunn-Irving, $\mu^{-1} = 2.6$; (e) Gunn-Irving, $\mu^{-1} = 2.2$. Experimental points are from Refs. 10 and 34.

form factor, one obtains the value 0.744 MeV = 2.65% small. We observe that the set of parameters $\mu_1^{-1} = 1.7$ F, $\mu_2 = 1.14\mu_1$ or the set $\mu_1^{-1} = 2.1$ F, $\mu_2 = 2.1\mu_1$ give only slightly different form factors, cross sections, and Coulomb energy. With the present accuracy, we cannot determine both μ_1 and μ_2 . We adhere to the first set of values as giving the best form factor.

Matching the mean-square radius means only that you have the correct initial slope to the form factor. As we see in curve e, this does not guarantee a good fit for larger q^2 . Thus we choose our parameters to match the form-factor curve at the expense of slightly incorrect initial slope and Coulomb energy. ψ_3 gives a radius of 1.75 F, 5.4% larger than the experimental value of 1.66 ± 0.07 F. Expressions for the radius and point Coulomb energy are given in the Appendix.

Having obtained the helium wave function and parameters we now discuss the cross section. We calculate in the center of mass and use the notation \mathbf{k} = photon wave vector, \mathbf{k}' = final proton wave vector, M = nucleon mass, $\boldsymbol{\rho}_j = \mathbf{r}_j - \mathbf{R}$ = nucleon position with respect to the c.m., g_j = gyromagnetic ratio, = 5.58 for proton ($j=1,2$), = -3.82 for neutron ($j=3$), \mathbf{A} = vector potential, $\mathbf{B} = \nabla \times \mathbf{A}$, $\mathbf{E} = -(1/c)\partial\mathbf{A}/\partial t$, and \mathbf{m}_j = magnetic moment of j th nucleon.

As mentioned before we consider the three interactions

$$V_A = - \sum_{j=1}^2 \frac{e}{M c} \mathbf{A}(\mathbf{r}_j) \cdot \mathbf{p}_j,$$

$$V_m = - \sum_{j=1}^3 \mathbf{m}_j \cdot \mathbf{B}(\mathbf{r}_j),$$

$$V_E = - \sum_{j=1}^2 e \mathbf{E}(\mathbf{r}_j) \cdot \boldsymbol{\rho}_j.$$

³⁴ C. DeVries, R. Hofstadter, A. Johansson, and R. Herman, Phys. Rev. 134, B848 (1964).

³⁵ K. Okamoto, Progr. Theoret. Phys. (Kyoto) 34, 326 (1965).

Our final spatial wave function is $U_f = U_D e^{ik \cdot \rho}$ and the initial is $U_H e^{-ik \cdot R}$, U_H being Ψ_1 , Ψ_2 , or Ψ_3 . The spin states have been specified. We use a plane wave photon. The differential cross section

$$d\sigma/d\Omega = (2\pi/\hbar)(\rho/F) |\langle f | V | i \rangle|^2,$$

where ρ = density of final states, F = incident flux, is to be summed over six final spins and averaged over two initial polarizations and two initial spins. The results are

$$\left. \frac{d\sigma}{d\Omega} \right|_{\mathbf{A} \cdot \mathbf{p}} = \frac{e^2 k k'}{4\pi M c^2 k} |B|^2 \sin^2 \theta, \quad (4)$$

$$\left. \frac{d\sigma}{d\Omega} \right|_{\mathbf{m} \cdot \mathbf{B}} = \frac{e^2 k k'}{48\pi M c^2} (|M_1 - M_2|^2 + \frac{1}{2} |M_1 - M_2 - M_3|^2 + |M_3|^2), \quad (5)$$

$$\left. \frac{d\sigma}{d\Omega} \right|_{\mathbf{E} \cdot \mathbf{r}} = \frac{e^2 M k k'}{4\pi \hbar^2} |E'|^2 \sin^2 \theta, \quad (6)$$

where

$$M_j = g_j \int d\tau U_f^* e^{ik \cdot \rho_j} U_H, \quad (7)$$

$$\mathbf{J} = \int d\tau U_f^* [e^{ik \cdot \rho_1} - \frac{1}{2} e^{ik \cdot \rho_2}] \nabla_\rho U_H, \quad (8)$$

$$= \hat{k}' B + \hat{k} X, \text{ which defines } B,$$

$$\mathbf{F} = \frac{2}{3} \int d\tau U_f^* [e^{ik \cdot \rho_1} - \frac{1}{2} e^{ik \cdot \rho_2}] \boldsymbol{\rho} U_H, \quad (9)$$

$$= \hat{k}' E' + \hat{k} X', \text{ which defines } E'.$$

θ is the c.m. angle of the outgoing proton. \mathbf{J} and \mathbf{F} are parallel to \hat{k} and \hat{k}' , but only $\boldsymbol{\varepsilon} \cdot \mathbf{J}$ and $\boldsymbol{\varepsilon} \cdot \mathbf{F}$ enter the expression for the cross section, and since $\boldsymbol{\varepsilon} \cdot \hat{k} = 0$, the

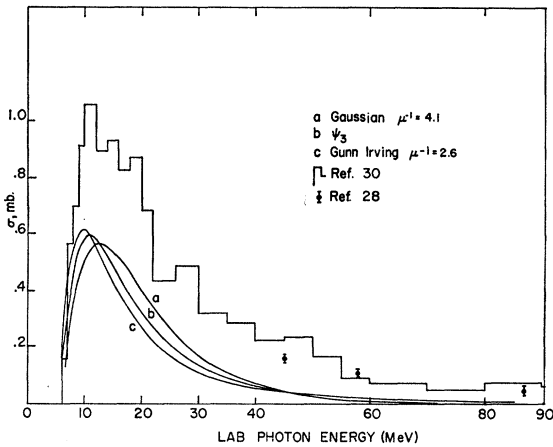


FIG. 2. Total cross section for the $\mathbf{A} \cdot \mathbf{p}$ interaction. Curve (a), Gaussian, $\mu^{-1}=4.1$; (b) Ψ_3 , $\mu_1^{-1}=1.9$, $\mu_2=1.44\mu_1$; (c) Gunn-Irving, $\mu^{-1}=2.6$. Experimental histogram is from Ref. 30. The points are from Ref. 28.

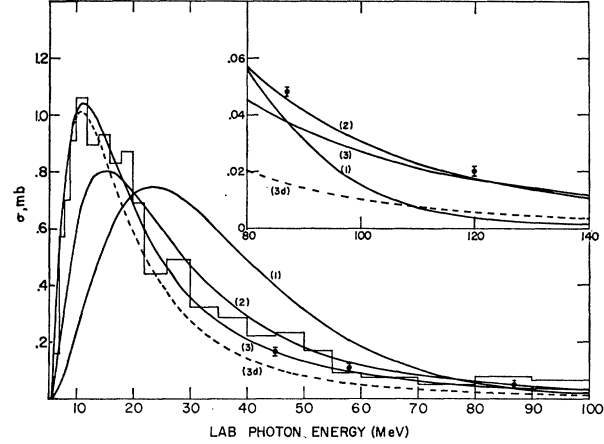


FIG. 3. Total cross section for the $\mathbf{E} \cdot \mathbf{r}$ interaction. Curve (1), Gaussian, $\mu^{-1}=4.1$; (2) Ψ_3 , $\mu_1^{-1}=1.9$, $\mu_2=1.44\mu_1$; (3) Gunn-Irving, $\mu^{-1}=2.6$; (3d) Gunn-Irving, $\mu^{-1}=2.6$, $e^{ik \cdot r}=1$. The histogram is from Ref. 30. The points are from Ref. 28.

part X parallel to \hat{k} is irrelevant. With the spin states we have used, these last six equations are correct for an arbitrary final three-nucleon spatial wave function $U_f(\boldsymbol{\rho}, \mathbf{s})$ and for any fully symmetric spatial wave function $U_H(\boldsymbol{\rho}, \mathbf{s})$ for the helium.

For the most part, the matrix elements M_j , B , E' are no harder to evaluate with $e^{ik \cdot \rho_j} \neq 1$, than in the dipole approximation. However, this causes a deviation from a $\sin^2 \theta$ distribution and the angular integration must be done numerically (for the Gunn-Irving wave function). For this we used the University of Illinois IBM 7094 computer.

III. RESULTS

In Fig. 2 are shown the total cross sections for the interaction $\mathbf{A} \cdot \mathbf{p}$ along with the data of Refs. 28 and 30. They are all nearly a factor of 2 too small at the peak, and a factor of 5 or more too small at higher energies.

Figure 3 shows the $\mathbf{E} \cdot \mathbf{r}$ results with the same wave functions. The Gaussian, curve (1), peaks at much too high an energy and at high energies drops off much too fast, as expected. Ψ_3 , curve (2), has a nearly correct high-energy behavior but is 20% too small at the peak and peaks at 16 MeV, about 4 MeV too high.

The Gunn-Irving wave function, curve (3), gives a surprisingly good fit to the data for all energies. The effect of setting $e^{ik \cdot r} = 1$ (dipole approximation) is shown by the dotted curve (3d). This dotted curve is then the same calculation as the early Gunn-Irving results,² with the exception that we have used the Hulthén deuteron wave function instead of the singular $r^{-1} e^{-\alpha r}$. The Hulthén wave function has the effect of raising the old results by a factor of about 1.3 at the peak and a somewhat larger factor at higher energies.

The results for the 90° cross section are shown in Fig. 4 for the $\mathbf{E} \cdot \mathbf{r}$ interaction. Only the Gunn-Irving wave function peaks at the proper energy and there it is

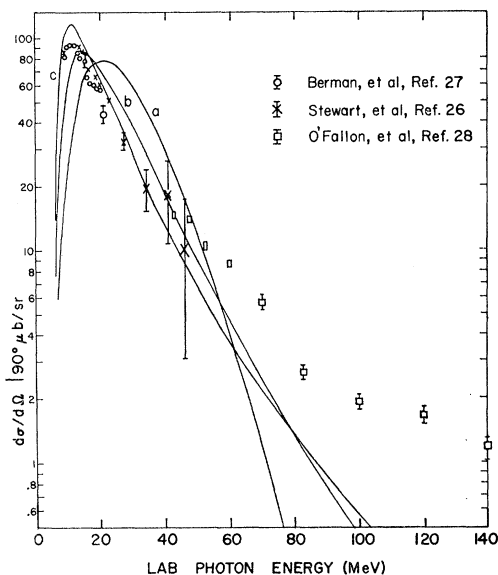


FIG. 4. Ninety degree differential cross section for the $\mathbf{E} \cdot \mathbf{r}$ interaction. Curve (a), Gaussian, $\mu^{-1}=4.1$; (b) Ψ_3 , $\mu_1^{-1}=1.9$, $\mu_2=1.44\mu_1$; (c) Gunn-Irving, $\mu^{-1}=2.6$. Experimental points are from Refs. 26, 27, and 28.

20% too high. The fact that the 90° results are much too small at high energies whereas the total cross section remains quite good is due to the forward peaking of the angular distribution, as shown in Fig. 5 at 60 MeV (curves 1 and 2). It practically disappears in the backward hemisphere and the peaking at 45° is greatly pronounced, in disagreement with experiment.

Also shown in Fig. 5 are the angular distributions for ψ_2 and ψ_3 using Foldy's interaction $\int_0^1 ds e^{i\mathbf{k} \cdot \mathbf{r}}$ (curves 1' and 2'), which gives a result intermediate between the dipole distribution ($\sin^2\theta$ in the center of mass) and the $\mathbf{E} \cdot \mathbf{r}$ results with the full retardation factor. This improves the angular distribution greatly but it is still too small in the backward hemisphere.

We also show in Fig. 5 the distribution from the $\mathbf{A} \cdot \mathbf{p}$ interaction (curve 3) for the Gunn-Irving wave function. For ease in comparison we have multiplied the actual theoretical result by 3.38 to normalize the curve to the 60° data point. The angular distribution is not greatly different from that of the Foldy interaction, but it is even smaller for large angles.

This fact, that the differential cross section agrees so poorly, indicates that we cannot take too seriously the agreement of the total cross at high energy. That a singular wave function which ignores mesons and produces an incorrect differential cross section should yield the correct total cross section at high energies must be regarded as somewhat fortuitous.

Of course the differential cross section is much more sensitive to the details of the wave function than is the total cross section. It would be very surprising if such a simple model as we are using were to correctly describe the details of the nucleus at an interaction energy of

say 60 MeV or greater, where short wavelengths begin to probe the internal structure. This means that the differential cross section at low or intermediate energies ($\lesssim 50$ MeV) is a sensitive test of the ground-state wave function. It is at the intermediate energies that various models will differ in their predictions sufficiently enough to be able to derive meaningful information from comparison with experiment. Accurate experimental differential cross sections in this energy range would be very helpful.

As mentioned in the Introduction, the final deuteron should have a radius which is smaller when the free proton is near and larger when farther away. Since our deuteron is more spread out than the helium, this correction would have the effect of increasing the overlap of the initial and final states, thereby increasing the cross section.

To qualitatively investigate the effect of a final-state interaction we have inserted a proton-deuteron square-well attraction of depth 75 MeV and radius 1.5 F. This increases the peak cross section by about 15% and decreases the high-energy ($\gtrsim 35$ MeV) cross section by nearly a factor of 2. The result is quite sensitive to the potential radius. The same low-energy effect has been noticed by Eichmann.⁴

These last results are encouraging, for they tend to bring the nonsingular wave function Ψ_3 into better agreement with the low-energy data. In fact, they will also tend to bring the $\mathbf{A} \cdot \mathbf{p}$ results into better agreement, although it is very doubtful that final-state interactions could account for nearly a factor of 2. The large difference between the two interactions is most likely due to the use of inexact wave functions.

We finally see that the three wave functions tried cannot match both the photodisintegration cross sec-

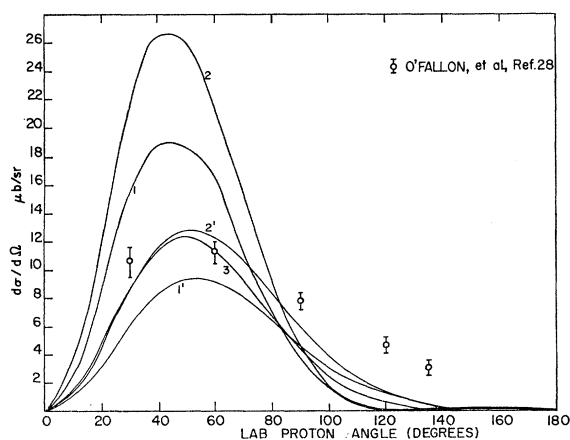


FIG. 5. Angular distribution at 60 MeV for three different interactions. Curves 1, 1', and 3 are the Gunn-Irving wave function Ψ_2 with $\mu^{-1}=2.6F$. Curves 2 and 2' are Ψ_3 with $\mu_1^{-1}=1.9F$, $\mu_2=1.44\mu_1$. Curves 1 and 2 are the interaction $\mathbf{E} \cdot \mathbf{r}$ with the full retardation factor $e^{i\mathbf{k} \cdot \mathbf{r}}$. Curves 1' and 2' are the $\mathbf{E} \cdot \mathbf{r}$ interaction with the Foldy space dependence $\int_0^1 ds e^{i\mathbf{k} \cdot \mathbf{r}}$ for the electric field. Curve 3 is the $\mathbf{A} \cdot \mathbf{p}$ interaction multiplied by 3.38 to normalize to the 60° data point. Experimental points are from Ref. 28.

tions and the ground-state properties of He^3 (especially the form-factor curves). In fact, they cannot even simultaneously match the ground-state quantities E_{Coulomb} , $\langle r^2 \rangle$, and form factors. Ψ_3 does best in this respect, giving a good fit to the form factor and E_{Coulomb} , and a slightly large $\langle r^2 \rangle$. The fact that Ψ_3 and the Gunn-Irving match well the high-energy total cross section without final-state interactions is not too significant, however, for the computed cross section should be low at high energies since virtual meson production does play a role which we have ignored. These meson currents cannot be neglected since the nucleon current interaction $\mathbf{A} \cdot \mathbf{p}$ gives too small results. This fact cannot be remedied by choosing better ground-state wave functions, for on the one hand they must have more high-momentum components to raise the cross section, while on the other hand they must have fewer high-momentum components to lower the form factors at high q^2 .

ACKNOWLEDGMENTS

The author gratefully acknowledges numerous helpful discussions with Professor D. G. Ravenhall, Professor L. J. Koester, and Professor J. H. Smith. He is also indebted to Dr. N. M. O'Fallon for the communication of her experimental results prior to publication. This calculation was initiated by Dr. N. M. O'Fallon as an analysis of her experimental results.

APPENDIX

We present here the expressions for the form factors, point proton Coulomb energy, and rms radius for the three functions (1), (2), (3).

If

$$g(\mu) = [1 + (q/\mu)^2/12] / [1 + (q/\mu)^2/18]^{3/2},$$

then the form factors are

$$F_1(q^2) = \exp\{-q^2/36\mu^2\},$$

$$F_2(q^2) = \frac{864}{(q/\mu)^4} [1 - g(\mu)],$$

$$F_3(q^2) = \frac{864}{(q/\mu)^4} N_f [2g(\frac{1}{2}(\mu_1 + \mu_2)) - g(\mu_1) - g(\mu_2)],$$

where

$$N_f = \left[1 + t^4 - 2 \left(\frac{2t}{1+t} \right)^4 \right]^{-1},$$

$$t = \mu_1/\mu_2.$$

The Coulomb energies $\langle \psi | e^2/r_{12} | \psi \rangle$ are

$$E_1 = 2 \left(\frac{3}{\pi} \right)^{1/2} e^2 \mu,$$

$$E_2 = \frac{16}{3\pi} \left(\frac{2}{3} \right)^{1/2} e^2 \mu,$$

$$E_3 = \frac{16}{3\pi} \left(\frac{2}{3} \right)^{1/2} e^2 \mu_1 N_f \left[1 + t^3 - 2 \left(\frac{2t}{1+t} \right)^3 \right],$$

and the rms radii computed either directly or by expanding the form factor are

$$\langle r^2 \rangle_1 = 1/6\mu^2,$$

$$\langle r^2 \rangle_2 = 5/9\mu^2,$$

$$\langle r^2 \rangle_3 = (5/9\mu_1^2) N_f \{ 1 + t^6 - 2[2t/(1+t)]^6 \}.$$